Int J Appl Earth Obs Geoinformation 88 (2020) 102063

Contents lists available at ScienceDirect

Int J Appl Earth Obs Geoinformation

journal homepage: www.elsevier.com/locate/jag

Space-time detection of deforestation, forest degradation and regeneration in montane forests of Eastern Tanzania

Eliakim Hamunyela[a,*], Patric Brandt[b,c], Deo Shirima[d], Ha Thi Thanh Do[b,e], Martin Herold[c], Rosa Maria Roman-Cuesta[b,c]

[a] University of Namibia, Faculty of Humanity and Social Sciences, Private Bag 13301, Windhoek, Namibia
[b] Center for International Forestry Research (CIFOR), P.O. Box 30677, 00100, Nairobi, Kenya
[c] Wageningen University & Research, Laboratory of Geo-Information Science and Remote Sensing, Droevendaalsesteg 3, PB Wageningen, 6708, the Netherlands
[d] Sokoine University of Agriculture, Department of Ecosystems and Conservation, Tanzania
[e] Forest Research Centre, Southern Cross University, Lismore, NSW 2480, Australia

ARTICLE INFO

Keywords:
Forest loss
Regeneration
Tanzania
Montane forest
SAGCOT

ABSTRACT

Naturally isolated montane forests in East Africa are hotspots of biodiversity, often characterised by high species endemism, and are fundamental contributors to water services. However, they are located in areas highly suitable for agriculture, making them a prime target for agricultural activities. The Eastern Arc Mountains (EAM) in Eastern Tanzania are within the target regions for agricultural development under the Southern Agricultural Growth Corridor of Tanzania (SAGCOT). However, forest monitoring initiatives that track long-term forest dynamics and the ecological impact of current agricultural development policies on forests, are lacking. Here, we use the STEF (Space-Time Extremes and Features) algorithm and Landsat time series to track forest disturbances (deforestation and degradation) and forest gains (regeneration) as spatio-temporal events over seventeen years (2001–2017) in the montane forests of the Mvomero District in Tanzania. We found that 27 % (~ 20 487 ha) of montane forests were disturbed between 2001 and 2017, mainly led by deforestation (70 %). Small-scale crop farms with maize, banana, and cassava crops, were the most planted on deforested areas. Most disturbances occurred at lower elevation (lowland montane), but there was an increasing shift to higher elevations in recent years (2011–2017). Forest disturbances exclusively occurred at small spatial scales, a pattern similar to other forest montane landscapes in Africa, which lowers detection capabilities in global forest loss products. Our locally calibrated and validated deforestation map (Producer's accuracy = 80 %; User's accuracy = 78 %) shows a gross underestimation of forest cover loss (> 10 000 ha) by global forest loss products in these mountainous forest landscapes. Overall, we found few areas undergoing forest regeneration, with only 9 % of the disturbed forest regenerating over 17 years. Long-term conversion to cropland prevented regeneration in the lowlands, with regeneration mainly happening at higher elevations. However, the shift of deforestation and forest degradation to higher elevations may challenge high elevation regeneration trends, leaving the remaining blocks of montane forest in the Mvomero District at a risk of degradation and disappearance. Without effective forest conservation measures, market-driven agricultural development is likely to trigger an expansion of cropland at the expense of forests to meet the increased demand for the agricultural products promoted, with negative impact on biodiversity, carbon sequestration and water services.

1. Introduction

Naturally isolated tropical forest landscapes such as montane forests are hotspots of biodiversity, often characterised by high species endemism (Burgess et al., 2007; Chaverri et al., 2016; Myers et al., 2000; Särkinen et al., 2012; Schmitt et al., 2010), but are vulnerable to human-induced disturbances, especially when they are located in areas highly suitable for agricultural production. Yet, montane landscapes often do not receive much attention from forest monitoring initiatives that track forest disturbances (deforestation and degradation), probably because of their small size. The focus is often on large lowland tropical forest ecosystems (Achard et al., 2014). Forest regeneration monitoring in montane forest landscapes is also scarce, leading to the paucity of information on the patterns and trends of regeneration after

* Corresponding author.
E-mail addresses: hamunyelae@unam.na, eliakimprof@yahoo.com (E. Hamunyela).

https://doi.org/10.1016/j.jag.2020.102063
Received 29 September 2019; Received in revised form 20 January 2020; Accepted 28 January 2020

disturbance in such forest landscapes.

The Eastern Arc Mountains (EAM), a range of unconnected blocks of mountains ranging from Southern Tanzania to Southern Kenya, are isolated montane forest landscapes which have a high level of plant and animal endemism. At least 800 vascular plant species and 96 vertebrate species found in EAM are endemic, and another 71 vertebrate species are near-endemic (Burgess et al., 2007; Lovett et al., 2001; Newmark, 1998; Lovett, 1998). Seventy one (71) vertebrates in EAM are threatened by extinction (Burgess et al., 2007). Apart from being a biodiversity hotspot, the EAM also play a vital role in the hydrological cycle, by being the main water catchment for important rivers (e.g. Wami River) in this area (Doggart and Loserian, 2007). However, these montane forests have been under human pressure for decades, resulting in complete disappearance of some of them (Hall et al., 2009). The EAM lost 25 % of the original forest extent to agriculture between 1955 and 2000 (Hall et al., 2009), and the remaining montane forests of EAM represent less than 30 % of the original forest extent (Burgess et al., 2007). Expansion of agricultural land for food and cash crops, for example tea (Jacobs et al., 2017) drove the disappearance of some of the EAM forest blocks (Hall et al., 2009).

With human population in East Africa still growing at a high rate (2.82 %), which is two times higher than the global rate (1.19 %; Gerland et al., 2014; United Nations, 2017), the demand for agricultural land to expand cropland and grazing areas is expected (Fisher, 2010). There has been effort over the years to protect montane forests in EAM by establishing forest reserves (Lovett and Moyer, 1992; Redhead, 1981), but forest disturbances still occur in these forest landscapes (Lyimo, 2014). Our understanding of the extent and trends of forest disturbance in EAM is however limited because continuous and elaborate monitoring of forest changes in these montane forest landscapes is lacking.

Global forest change datasets generated from satellite data (e.g. Landsat data) provide annual information on forest loss and gain (Hansen et al., 2013), but the utility of such information for local forest change assessment in Afro-montane forest landscapes is not known. However, evidence from elsewhere show that global forest change datasets substantially underestimate forest loss (Milodowski et al., 2017; Tropek et al., 2014). Forest loss caused by small-scale disturbances were particularly found to have high likelihood of being underestimated by globally or regionally generated forest change datasets (Milodowski et al., 2017). In many African forest landscapes, forest disturbance occurs on small spatial scale (Fisher, 2010; DeVries et al., 2015a; Tyukavina et al., 2018), making the underestimation of forest loss by global or regional forest change datasets in these landscapes highly likely. Underestimation of forest loss would consequently leads to underestimation of forest regeneration because only areas where forest loss is detected would be assessed for forest regeneration. To improve our understanding of forest disturbance and regeneration dynamics in Afro-montane forest landscapes, locally calibrated forest change datasets are needed.

In recent years, a number of studies analysed forest cover change in some Afro-montane forests using locally calibrated algorithms (e.g. Brandt et al., 2018; DeVries et al., 2015a; Hall et al., 2009; Hamunyela et al., 2017), but these studies only focused on forest disturbance, thus ignoring forest regeneration after disturbance. Detection of forest regeneration after disturbance is generally scarce because concurrent mapping of forest disturbance and regeneration remains limited in satellite-based forest monitoring. This is mainly because development of algorithms for automated forest regeneration detection has been limited compared to forest disturbance. Yet, detecting both forest disturbance and regeneration makes accounting of net forest greenhouse gas (GHG) emissions possible. It also allows for the profiling of forest disturbance pathways in regard to certain drivers, and information on forest regeneration is particularly important under current restoration initiatives such as AFRI100 (the African Forest Landscape Restoration Initiative).

The use of dense time series of satellite data, rather than annual time series, for forest monitoring in recent years has improved the detection of forest disturbance and regeneration (DeVries et al., 2015b), but accurate detection of small-scale and low-magnitude forest disturbances is still challenging (Milodowski et al., 2017) particularly in seasonally dry forests where strong seasonality complicates the detection of forest cover changes. Some montane forests in East Africa, including Tanzania, have strong seasonality in their photosynthetic activity and canopy water content (DeVries et al., 2015a), and forest disturbances in these forest landscapes mainly occur at small spatial scales (Brandt et al., 2018). Strong seasonality makes it difficult for the widely used single-time series change detection algorithms (e.g. BFASTmonitor -Breaks For Additive Season and Trend Monitor (Verbesselt et al., 2012) and CCDC - Continuous Change Detection and Classification (Zhu and Woodcock, 2014a,2014b)) to differentiate small scale forest disturbances from natural intra-annual variations.

Recently, a new algorithm (STEF - Space-Time Extremes and Features: https://github.com/hamun001/STEF) that combine spatial and temporal context has been developed to enhance detection of small-scale and low-magnitude forest disturbances in dry forests with strong seasonality from time series of satellite data (Hamunyela et al., 2017; Brandt et al., 2018). STEF leverages both spatial and temporal information in satellite data to enhance the detection of forest changes, and has been extended to support concurrent mapping of forest disturbance and regeneration. With STEF algorithm, the *STEFmonitor* function provides the capability for forest disturbance detection, whereas the *STEFregrowth* function detects forest regeneration after disturbance. Up to now, however, the application of STEF had been limited to tracking forest disturbances (deforestation and degradation) in a few countries in Eastern Africa (Ethiopia, and Kenya), whereas forest regeneration had not yet been assessed. Here, we apply STEF to assess forest disturbance and regeneration patterns and trends in the evergreen and seasonally dry montane forest landscapes located in the Mvomero District, Tanzania. Montane forest blocks in Mvomero District are part of the biologically rich EAM. We address the following research questions:

a) What has the forest disturbance pattern been for montane forests in Mvomero District, Tanzania between 2001 and 2017? How have the patterns varied across time and along elevation?
b) What are the main drivers of forest disturbance in the montane forest landscapes of Mvomero District?
c) Do these forests regenerate after forest disturbance? How does regeneration vary across along elevation?

We focused on Mvomero District in Morogoro Region, Tanzania (Fig. 1) where smallholder farming is the primary activity in the District, consisting of crop production and livestock keeping mainly in the form of pastoralism (Robinson et al., 2014). We defined deforestation as the conversion of a forest area to non-forest area (Hansen et al., 2013), whereas forest degradation was defined as partial removal of forest, but the area remained forest. Forest regeneration was defined as re-establishment or recovery of forest canopy after disturbance.

2. Study area

Our study area covers two of the 13 blocks that make up the EAM: Nguru and Uluguro Mountains located in Mvomero District in Morogoro Region, Tanzania (Fig. 1). The EAM are 13 separate mountain blocks located in Kenya and Tanzania. The elevation ranges from 200 m to 2 637 m above the sea level. Nguru and Uluguru mountains form the main water catchment of the Wami River (Doggart and Loserian, 2007), which supports the livelihood of many people within the Wami river basin, and is an important source of water for wildlife in this area (Tobey, 2008).

Climatic conditions in these areas are predominantly influenced by

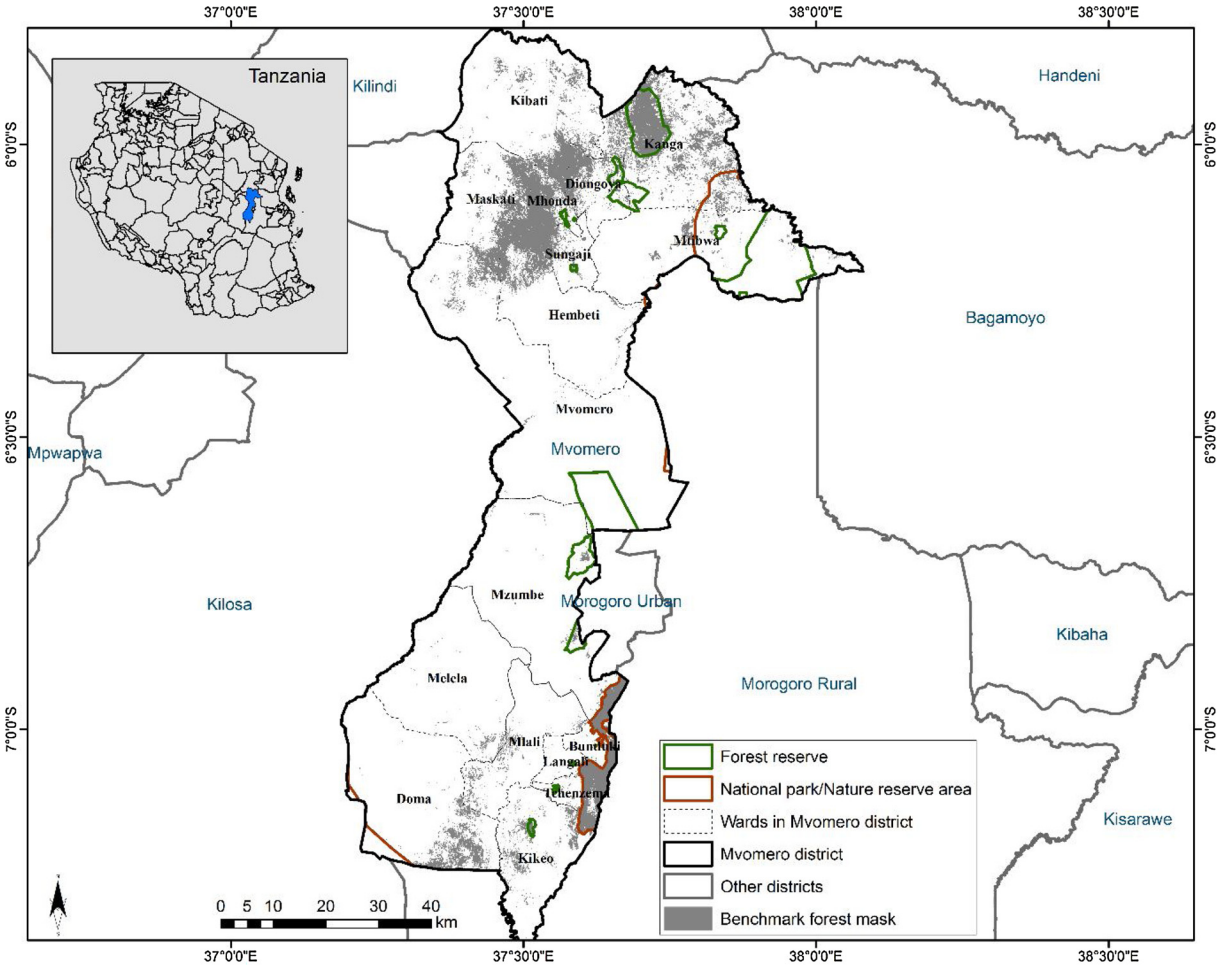

Fig. 1. The location of the Mvomero District in Tanzania, as well as the spatial distribution of forest within the District. Forest reserve and National park/Nature reserve data were acquired from the World Database of Protected Areas (UNEP-WCMC, 2019).

the Indian Ocean (Pócs et al., 1990; Newmark, 2002; Doggart and Loserian, 2007), but the eastern and western sides of Nguru and Uluguru mountains receive different rainfall amounts. Rainfall on eastern slopes ranges from 2100 to 4000 mm/year, and from 1000 to 2000 mm/year for western slopes (Pócs et al., 1990). These mountainous areas receive rainfall throughout the year. The wettest period is March-April, whereas the June to August is the least wet period (Pócs et al., 1990; Doggart and Loserian, 2007). Besides commercial cropland area in the lowlands whose products are nationally distributed, smallholder mixed crop-livestock farming is also prominent in these montane regions (Robinson et al., 2014). Through Southern Agricultural Growth Corridor of Tanzania (SAGCOT) initiative, the Government of Tanzania is promoting profitable smallholder farming by incentivising stronger linkages between smallholders and commercial agribusinesses (United Republic of Tanzania, 2011). There has been a large increase of livestock in our study area due to immigration of pastoralists from other regions (Raben et al., 2006; Lyimo, 2014). Large-scale droughts in recent years in Tanzania have been pushing pastoralists from drier surrounding areas to wetter areas like Nguru and Uluguru (Lyimo, 2014).

3. Data and methods

The overview of the methods applied in this study to track forest disturbance and regeneration from Landsat time series is shown in Fig. 2. First, we pre-processed Landsat multi-spectral and normalised difference moisture (water) index (NDMI; Gao, 1996) images, and generated a benchmark forest mask (see Section 3.1). NDMI is calculated as a ratio between the NIR (Near Infrared) and SWIR (Shortwave Infrared) whereby NDMI = (NIR - SWIR) / (NIR + SWIR). Second, we detected spatio-temporal anomalies in Landsat NDMI time series after spatial normalisation, and subsequently extracted space-time features (see Section 3.2). Third, we predicted forest disturbance from space-time features (see Section 3.3). Fourth, we classified forest disturbances and detected forest regeneration (see Section 3.4). Fifth, we ground validated the forest disturbances and regeneration, and subsequently determined the follow-up land-use after deforestation (see Section 3.5). Sixth, we related forest disturbances to elevation (see Section 3.6). Seventh, we compared our deforestation map with a widely used existing global forest loss product (Hansen et al., 2013; see Section 3.7).

3.1. Remote sensing data acquisition and pre-processing

We downloaded and pre-processed Tier 1 Landsat-5/TM, Landsat-7/ETM + and Landsat-8/ OLI surface reflectance data and their corresponding NDMI images, covering the period of 1990–2017, from The United State of America's Geological Survey (USGS) Landsat surface Reflectance (SR) Climate Data Records (https://espa.cr.usgs.gov/). Tier 1 Landsat scenes refer to the Landsat data that have the highest data quality and are suitable for time-series analysis because they have good geometric accuracy. Landsat-5/TM and Landsat-7/ETM + surface reflectance products were generated using the standard Landsat Ecosystem Disturbance Adaptive Processing System (LEDAPS) algorithm (Masek et al., 2006; Schmidt et al., 2013), whereas the Landsat 8

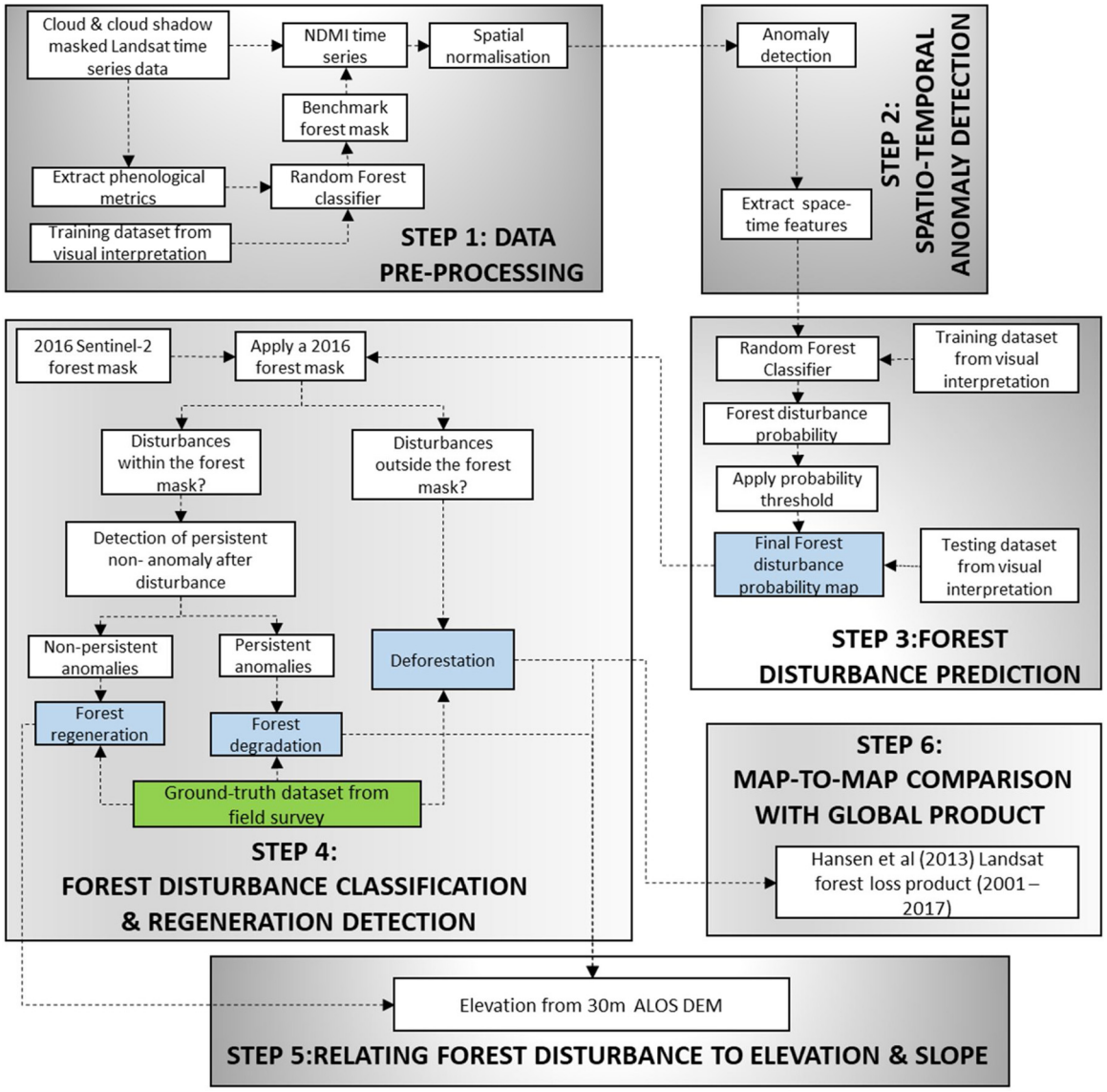

Fig. 2. The workflow followed to map forest disturbance and regeneration in Mvomero District, Tanzania, using Landsat time series and STEF algorithm.

Table 1
The proportion forest cover at each elevation zone in Mvomero District based on the benchmark forest mask. Elevation zones are based on Hall et al. (2009). The elevation was derived from Advanced Land Observing Satellite (ALOS) Digital Surface Model (AW3D30).

Elevation zone	Elevation (m)	Proportion of forest pixels (%)
Lowland montane	200–800	36.4
Submontane	800–1 200	20.6
Montane	1 200–1 800	26.9
Uppermontane	> 1 800	16.1

OLI surface reflectance products were generated using the Landsat 8 OLI surface reflectance algorithm (Vermote et al., 2016). Clouds and cloud shadows in Landsat data were masked using the pixel quality flags which were distributed together with Landsat surface reflectance products. The pixel quality flags were generated using the CFmask algorithm (Zhu et al., 2015; Zhu and Woodcock, 2012, 2014a,2014b). Only pixels which were flagged as clear - not contaminated by atmospheric artefacts, based on pixel quality information, were not masked. We also masked non-forest areas using a benchmark forest mask (year 2000) to avoid confusing changes occurring in non-forest areas (e.g. crop harvest) with forest disturbances. A benchmark forest mask was created by classifying the study area into forest and non-forest areas using a random forest classifier (Breiman, 2001) implemented in the randomForest R-package (Liaw and Wiener, 2002). The inputs into the classifier were metrics (temporal median, standard deviation, coefficient of variation, the 25th and 95th percentiles, and the seasonal amplitude - the difference between 25th and 95th percentile) computed per pixel from 1990 to 2000 Landsat time series of the Blue, Green, Red, Near Infrared, Shortwave Infrared, Thermal spectral bands and the NDMI. The classifier was trained using visually interpreted forest (n = 5000 pixels) and non-forest (n = 5000 pixels) reference data, selected through simple random sampling. Areas classified as forest were further pre-processed to remove forest patches smaller than 0.5 ha, to conform to the Tanzanian areal definition of a forest (United Republic of Tanzania, 2018). The final benchmark forest mask consisted of 75 735.36 ha of forest. Table 1 shows the proportion of forest at each elevation zone in Mvomero District, based on the benchmark forest mask.

Forests in the lowland montane of the study area are characterised by strong seasonal variation in its photosynthetic activity and leaf water content. Strong seasonal variations in satellite image time series should be accounted for during forest disturbance detection to minimise false

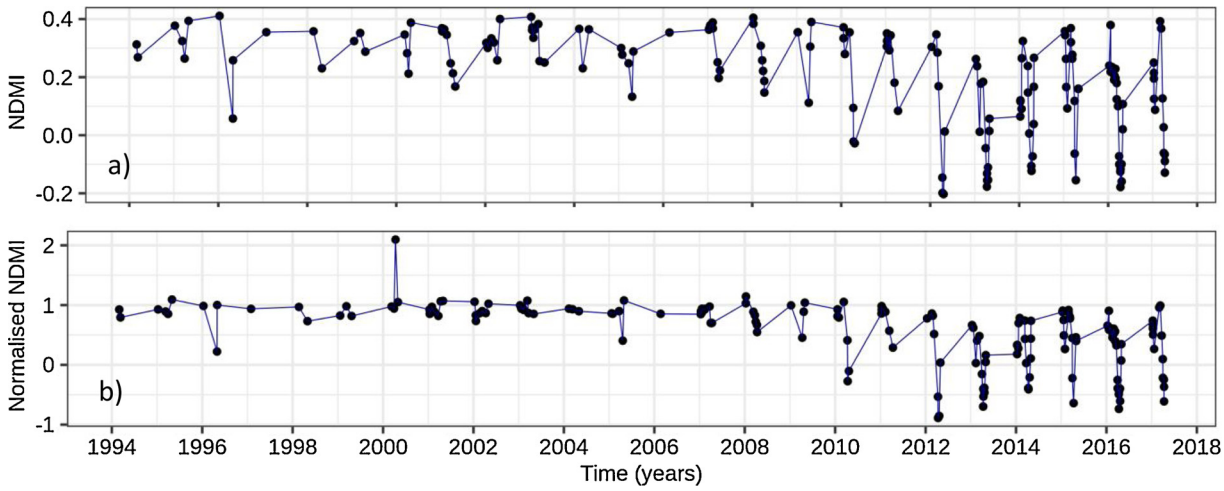

Fig. 3. An example of (a) the original and (b) spatially normalised pixel-time series for Landsat normalised difference moisture index (NDMI) from montane forest in the Mvomero District, Tanzania. The forest at this pixel was disturbed between 12 March 2010 and 10 April 2010.

detections and reduce omission of real changes (Hamunyela et al., 2016a). Differences in spectral resolution among Landsat sensors also propagate inter-sensor differences in the time series (Roy et al., 2016) that may negatively affect detection of forest disturbances. We spatially normalised NDMI time series to reduce seasonal variations (Hamunyela et al., 2016a). Hamunyela et al. (2016a) used 95th percentile value computed from a local moving window around the target pixel to normalise the value of the target pixel. Unlike Hamunyela et al. (2016a), here we used zonal spatial normalisation approach to increase computational efficiency. To do this, the study area was first classified into phenologically unique forest zones. Next, each pixel value in each NDMI image was normalised using the 95th percentile value computed from all pixel values in its respective phenological zone. The K-mean clustering method (k = 10, Hartigan, 1975) was used to classify the forest into phenologically unique zones. The inputs into the K-mean classifier were temporal median, standard deviation, coefficient of variation, 25th and 95th percentiles and the seasonal amplitude (difference between 25th and 95th percentiles) metrics also computed per pixel from the 1990–2000 NDMI time series.

Fig. 3 shows an example of NDMI pixel-time series before and after spatial normalisation. Note that phenological variation is not clearly defined even prior to spatial normalisation (Fig. 3a), however the variability prior to disturbance has been reduced in Fig. 3b. At this pixel, there were too few clear Landsat observations per year to clearly capture phenological variation of the forest. The average number of clear observations per year between 1990 and 2017 was only 10. Yet, each Landsat sensor has 16-day revisit. Clear observations are few because these montane areas are frequently covered by cloud. Also note that spatial normalisation does not only reduce seasonal variations; it also maximises the difference between the mean value of the observations before the disturbance and the value at the disturbance, thus increasing the detectability of disturbances (Hamunyela et al., 2016a). In Fig. 3a, for example, the absolute difference between the mean value of the observations before the disturbance and the value of the observation at the disturbance (disturbance date: 10 April 2010) was 0.46. This difference, however, increased to 1.53 after spatial normalisation (Fig. 3b).

3.2. Spatio-temporal anomaly detection

We detected spatio-temporal negative anomalies from spatially normalised NDMI time series using STEF*monitor* algorithm (Hamunyela et al., 2017, 2016a, b) implemented in STEF R-package (https://github.com/hamun001/STEF). We chose NDMI because it is better suited for forest cover change than other in vegetation indices (DeVries et al., 2015b). Spatio-temporal negative anomalies were tracked between 2001 and 2017 while using the NDMI observations from 1990 to 2000 as a reference. An observation was classified a spatio-temporal negative anomaly if it was smaller than the percentile threshold computed over the reference period (history period) of a local data cube. A local data cube was defined around the target pixel, and had both a spatial and temporal extent, which were user-defined. A temporal extent corresponded to the length of the NDMI time series (1990–2017). The spatial extent was set to 11 by 11 Landsat pixels (~ 10.9 ha). This spatial extent was considered sufficient because the change processes in our study area occurred on a small spatial scale and our reference period was long enough to derive a stable percentile threshold (see Hamunyela et al., 2016b). A 5th percentile threshold was used to identify negative anomalies because it leads to accurate detection of forest disturbances especially in areas where disturbances occur at small spatial scale and have a low-magnitude of change (Hamunyela et al., 2017, 2016b). A pixel was flagged potentially disturbed if there were two consecutive negative spatio-temporal anomalies. Once two consecutive spatio-temporal negative anomalies were detected, STEF*monitor* function extracted a set of space-time features from the local data cube, which were then used later on to predict forest disturbances (Hamunyela et al., 2017). The space-time features were then used as predictors of forest disturbance (see Section 3.3).

3.3. Forest disturbance prediction and validation

We computed forest disturbance probability at each pixel using space-time features as predictors of forest disturbance. The probability of forest disturbance was calculated using random forest algorithm (Breiman, 2001). The random forest model was trained with 208 sample pixels (disturbed forest = 124, stable forest = 84) generated through a simple random sampling approach from pixels with two consecutive negative spatio-temporal anomalies (see Section 3.2). The training sample pixels were visually interpreted using high spatial resolution imagery available in Google Earth™ (https://www.google.com/earth/) and Bing Maps (http://www.bing.com/maps/), which were complemented with all available Tier 1 Landsat multi-spectral image time series, following the timesync approach proposed by Cohen et al. (2010). Fig. 4 shows an example of forest cover loss between 07 August 2012 and 23 October 2016 in Mvomero District as captured by high resolution images in Google Earth™. Next, we used a probability threshold of 0.25, which achieved the smallest difference (lowest area bias) between producer's and user's accuracy, to discriminate false detections from forest disturbances. This probability threshold was determined using the training samples. The study area was then classified

Fig. 4. An example of forest cover loss in Mvomero District of Tanzania, as visible from high resolution images in Google Earth™. Images were acquired on 07 August 2014 (left image) and 23 October 2016 (right image).

into two strata: disturbed and stable forest area stratum. The proportion for disturbed forest stratum was 29.6 % whereas the stable forest stratum was 70.4 %. A total of 421 reference sample pixels (disturbed forest = 186 and stable forest = 235) generated through stratified probability sampling (Stehman, 2009) were used to assess the accuracy of the forest disturbance map. The reference data was acquired through visual interpretation of 30 m Landsat multi-spectral image time series and high spatial resolution imagery available in Google Earth™ (https://www.google.com/earth/) and Bing Maps (http://www.bing.com/maps/). The allocation of the sample size to each stratum was based on the approach recommended by (Olofsson et al., 2014; Stehman et al., 2012), which ensures a reliable estimation of overall accuracy, producer's and user's accuracy for classes with small area proportions. Next, we calculated area-adjusted producer's accuracy (PA) and user's accuracy (UA) for forest disturbance.

3.4. Forest disturbance classification and regeneration detection

To understand the current status of the disturbed forest areas, we classified disturbed areas into deforestation, forest degradation and regeneration (Fig. 2; Step 4). A disturbed forest area was classified i) as deforested if it was no longer covered by forest, ii) as degraded if the forest was partially removed, but the area remained forested, and iii) regenerating if the forest was recovering from the impact of disturbance. To identify deforested areas, we applied a Sentinel-2 forest mask of 2016 (http://2016africalandcover20 m.esrin.esa.int/) to the forest disturbance map. Disturbed areas which were not within the Sentinel-2 forest mask of 2016 were considered to have remained non-forest after disturbance, hence were deforested. For disturbed areas that were within the Sentinel-2 forest mask of 2016, we considered them either to be degraded or regenerating after a disturbance event occurred.

We disentangled regenerating forest from degraded forest by applying a forest regrowth monitoring algorithm (*STEFregrowth*) also implemented in the STEF R-package (https://github.com/hamun001/STEF) to track forest regeneration on the disturbed forest areas that were within the 2016 Sentinel-2 forest mask. *STEFregrowth* detects forest regeneration after disturbance from satellite time series by assessing whether previously anomalous observations in the time series of a target pixel ceased to be spatio-temporal negative anomalies over a user-defined time frame until the end of the time series. Here we used 1.5 years as the minimum time-frame that non-anomalous status should persist before flagging a previously disturbed forest pixel as forest regeneration. We used 1.5 years as minimum time-frame to minimise chances of confusing cropland dynamics with forest regeneration. Similar to forest disturbance detection (see Section 3.2), the percentile threshold for determining whether an observation was anomalous or not after disturbance was computed from the reference period of a local data cube, and was similar (5^{th} percentile) to the one used to identify anomalies in Section 3.2. The spatial and temporal extent of the local data cube were also similar to those used for tracking spatio-temporal anomalies (see Section 3.2). Pixels that were located within the Sentinel-2 forest mask of 2016 and where observations persistently ceased to be anomalous for a minimum of 1.5 years until the end of the time series were classified as forest regeneration. Disturbed forest areas where no forest regeneration was detected by *STEFregrowth* were subsequently classified as forest degradation.

3.5. Ground validation of deforestation, forest degradation and regeneration

We conducted a field data collection in the summer of 2018 (July/August) to ground validate deforestation, forest degradation and regeneration maps produced from satellite data (Section 3.4). Due to time and field data collection cost, the field campaign only focused on Nguru Mountains, in the northern part of Mvomero District (Fig. 5) were most of deforestation, forest degradation and regeneration were detected. Four sampling sites (Fig. 5) were purposely selected to target areas with varying rates of deforestation, forest degradation, regeneration, and cattle density (based on Robinson et al. (2014)) to ensure that they are representative of the entire study area. We also ensured that sampling sites cover different wards. Tanzania is sub-divided into various administrative divisions, of which a ward is one of the lowest administrative division. Similar to Brandt et al. (2018), each sampling site had a radius of 5 km. Within each sampling site, we selected pixels from deforestation, forest degradation and regeneration strata using stratified probability sampling approach (Stehman, 2009). In total, 217 sample pixels were selected within these four sampling sites. Out of 217 samples, 112 were from deforestation stratum, 105 from forest degradation and 51 were from forest regeneration stratum. We used open data kit (ODK) to collect locational and thematic information at each sample pixel, including the current land use/land cover, and presence/absence of fire relics and signs of livestock grazing and browsing. In cases where a deforested pixel was converted to cropland, we also documented the crops that we found being grown on a deforested pixel. The field data were then used to calculate the producer's accuracy (PA) and user's accuracy (UA) of deforestation, forest degradation and forest regeneration maps. The information on the follow-up land use/cover after deforestation was used to identify the main drivers of deforestation (Fig. 2; Step 4).

3.6. Relating deforestation, forest degradation and regeneration to elevation

We assessed how deforestation, forest degradation and regeneration varied with elevation over the years in the montane forests of Mvomero District (Fig. 2; Step 5). To do this, we overlaid the 30 m resolution ALOS Digital Surface Model (AW3D30, provided by the Japan Aerospace Exploration Agency: https://www.eorc.jaxa.jp/ALOS/en/aw3d30/index.htm) with deforestation, forest degradation and regeneration maps. We classified elevation into 4 zones, namely: lowland montane (200–800 m), submontane (800–1200 m), montane (1200 − 1800 m) and uppermontane (> 1800 m). Next, the mapped

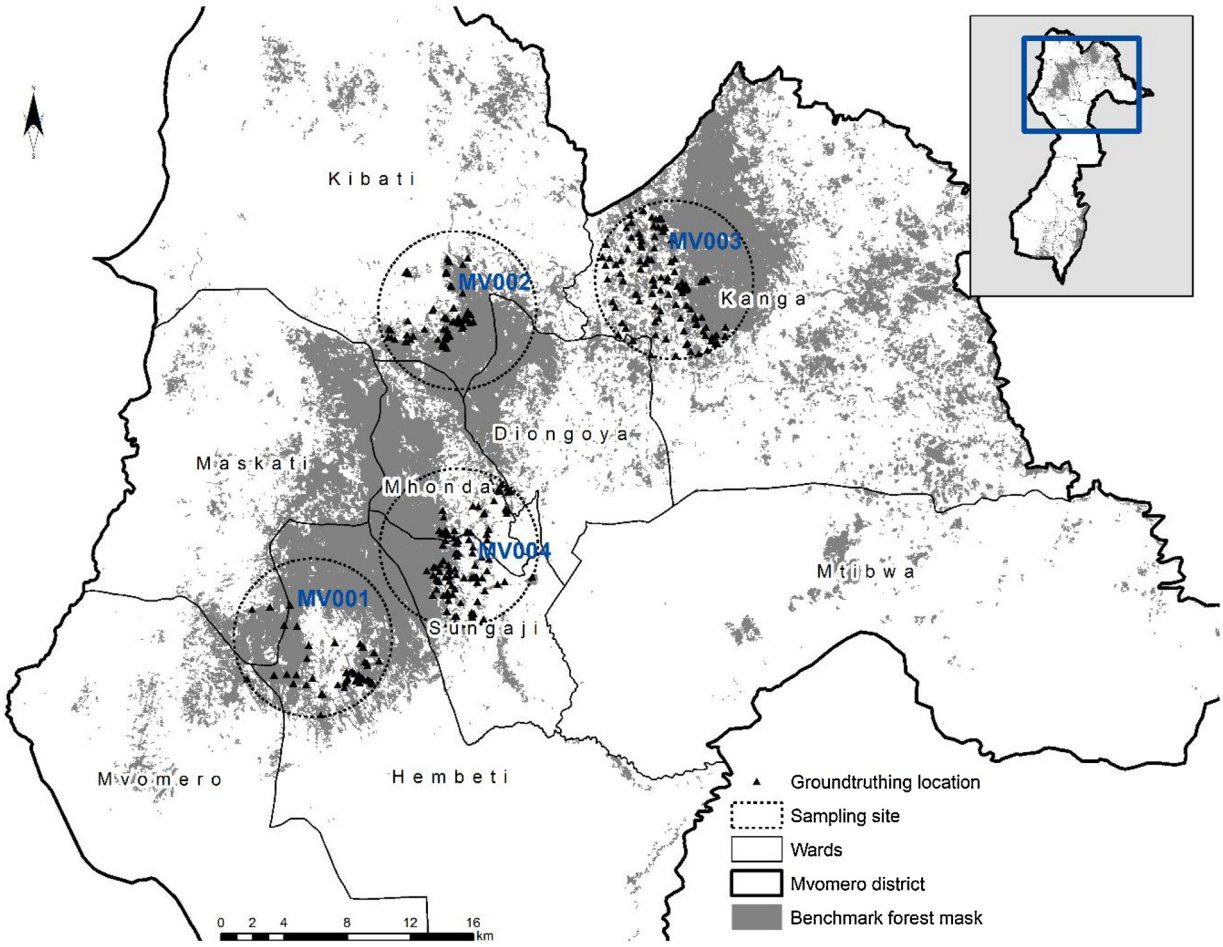

Fig. 5. The location of four sampling sites where field verification campaign took place. Each sampling site has a radius of 5 km.

areas of deforestation, forest degradation and regeneration were computed per elevation zone. To assess whether there has been elevational shift in forest disturbance over the years, we grouped the deforestation and forest degradation into two temporal categories, namely the 2001–2010 and 2011–2017. For each temporal category, we calculated the proportion of deforested and degraded Landsat pixels at each elevation zone. We also calculated forest regeneration success at each elevation zone. Forest regeneration success was defined as the total area of regenerated forest at a particular elevation zone divided by the total area of forest disturbed at the same elevation zone.

3.7. Comparison to global forest loss product

We compared our locally calibrated deforestation map with a global forest loss dataset (Hansen et al., 2013) using a map-to-map comparison approach to assess whether globally generated forest loss datasets can provide reliable forest change information in complex montane forest landscapes (Fig. 2; Step 6). The global forest loss dataset was generated from Landsat data using a globally tuned decision tree algorithm (Hansen et al., 2013), and is freely available annually since 2000 (http://earthenginepartners.appspot.com/science-2013-global-forest). To ensure consistency, the comparison of forest loss datasets was limited to the changes that occurred within the benchmark forest mask, produced in Section 3.1.

4. Results and discussion

4.1. Forest disturbance and regeneration across Mvomero District

Montane forests of the Mvomero District underwent frequent small-sized forest disturbances between 2001 and 2017 that have resulted in large areas of forest loss (Fig. 6). An estimated 20,487 ha of forest (27 % of the benchmark forest mask: 75,735 ha) were deforested (14 341 ha) and degraded (6 146 ha) during our study period. This pattern of small-sized forest disturbances is similar to other montane regions in Eastern Africa (Ethiopia and Kenya) (Devries et al., 2016; Pratihast et al., 2014; Brandt et al., 2018). We were able to map these small-sized forest disturbances with producer's and user's accuracy of 70 % and 69 %, similar to those achieved in Mau Forest in Kenya using STEF algorithm (Brandt et al., 2018). Despite the complex temporal dynamics before and after forest disturbance (Fig. 7), we were also able to detect deforestation, forest degradation and regeneration concurrently with high spatial accuracy (around 70 %; Table 2). This high spatial accuracy could be attributed to the fact that we used a method that leverages spatial and temporal information in satellite data to detect forest disturbance and regeneration. Spatial and temporal contexts provide complementary information that can enhance automated identification of land cover changes (Hamunyela et al., 2016a; Zhu, 2017). Our spatio-temporal method therefore offers new prospects for incorporation of forest regeneration into forest change assessments especially in forest landscapes with strong seasonality. Forest degradation and regeneration maps had the highest area bias (Table 2), mainly because separating degradation and regeneration is more challenging when compared to deforestation.

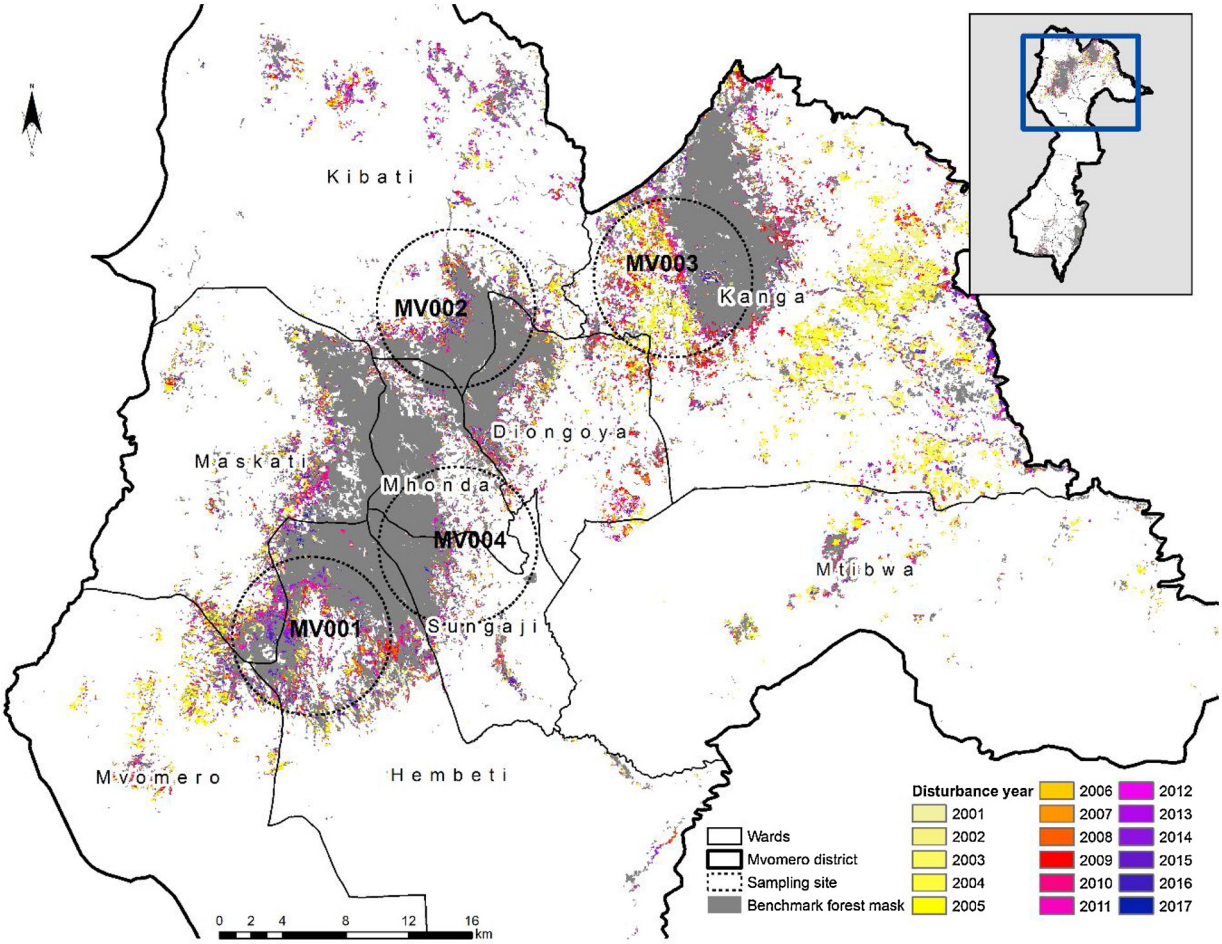

Fig. 6. Forest disturbance by year in the Mvomero District, Tanzania as detected from Landsat time series (2001–2017) using STEF (Space-time Extremes and Features) algorithm (Hamunyela et al., 2017).

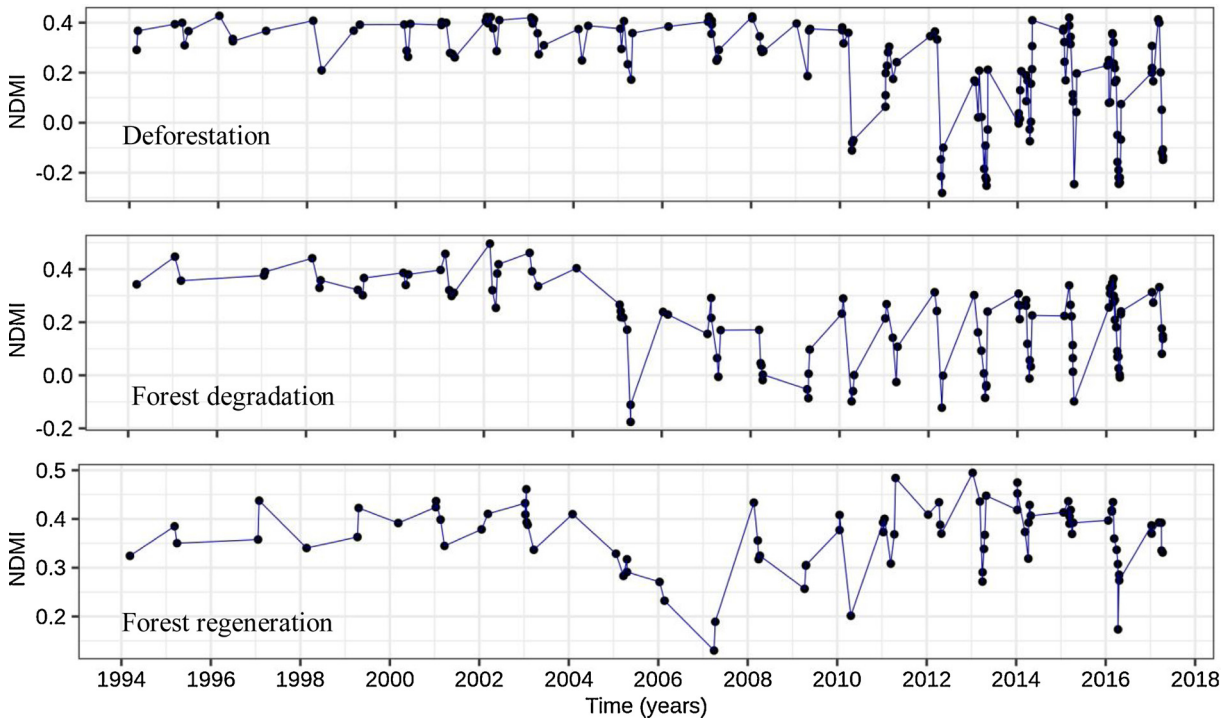

Fig. 7. Landsat normalised difference moisture index (NDMI) time series of a deforested, degraded, and regenerated pixels of a montane forest in Mvomero district, Tanzania.

Table 2
Producer's (PA) and User's (UA) accuracy, and area bias, for deforestation, forest degradation and regeneration detected in montane forest in Mvomero district, Tanzania.

	PA[%]	UA[%]	Area bias[%]
Deforestation	80	78.2	1.8
Forest degradation	78.7	72.5	6.2
Forest regeneration	70.6	75	−4.4

Forest disturbance in the Mvomero District was driven by deforestation (Fig. 8). Groundtruthing revealed that most of the deforested area (94 %) was converted into cropland for food crops. Our groundtruthing exercise recorded a diversity of crops (13 crop types) planted on deforested areas. Bananas, cassava and maize were the most planted crops (Fig. 9). A previous studies also found these crops to be among the most planted in this area. Some crops (e.g. Cardamom and Cacao) planted in our study area are shade tolerant (they need a proportion of forest cover to cultivate), whereas crops such as maize, beans, and others are shade intolerant (need 100 % forest cover removal) (Mwampamba and Schwartz, 2011). Our results show that small-scale crop farming could be the main driver of deforestation in the montane forest landscapes of Mvomero District. This is not surprising because agriculture is known to drive 83 % of deforestation in the tropics (Fisher, 2010; Hosonuma et al., 2012; Carter et al., 2015; Tyukavina et al., 2018). Our study area is within the target regions for agricultural development under the Southern Agricultural Growth Corridor of Tanzania (SAGCOT). The SAGCOT initiative promotes agricultural development by smallholder farmers through access to the market. Therefore, agriculture-driven forest loss in our study area in recent years might be, in part, relate to the SAGCOT initiative, despite environmental sustainability being a priority for the SAGCOT initiative. Thus, without effective conservation measures, market-driven agricultural development is likely to trigger an expansion of cropland at the expense of forests to meet the increased demand for the agricultural products promoted. To mitigate unintended effects on forests, agricultural development policies should actively incentivise sustainable intensification (e.g. increased farm productivity and profitability) to avoid triggering unintended expansion of agricultural land into natural ecosystems (Brandt et al., 2018; Carter et al., 2015). Immigration of pastoralists from drier surrounding areas to wetter areas like Nguru and Uluguru mountains in search for water and pasture during droughts (Raben et al., 2006; Lyimo, 2014) might also have contributed to forest disturbance in our study area. Intensification practices for both crops and livestock would help reducing unintended forest disturbances in montane forest landscapes of Mvomero District. However, intensification is often accompanied by increased use agrochemical inputs, which could have detrimental effects on the environment. Therefore conservation agriculture might be a better option for attaining increased food production while conserving forests.

The remaining 30 % of forest loss in Mvomero District was related to forest degradation. However, forest degradation was probably underestimated since degradation events tend to be too small to be detected with 30 m resolution Landsat data (Brandt et al., 2018). In part, forest degradation in our study area was probably driven by the cultivation of shade tolerant crops (e.g. cardamom, cacao) that need a proportion of

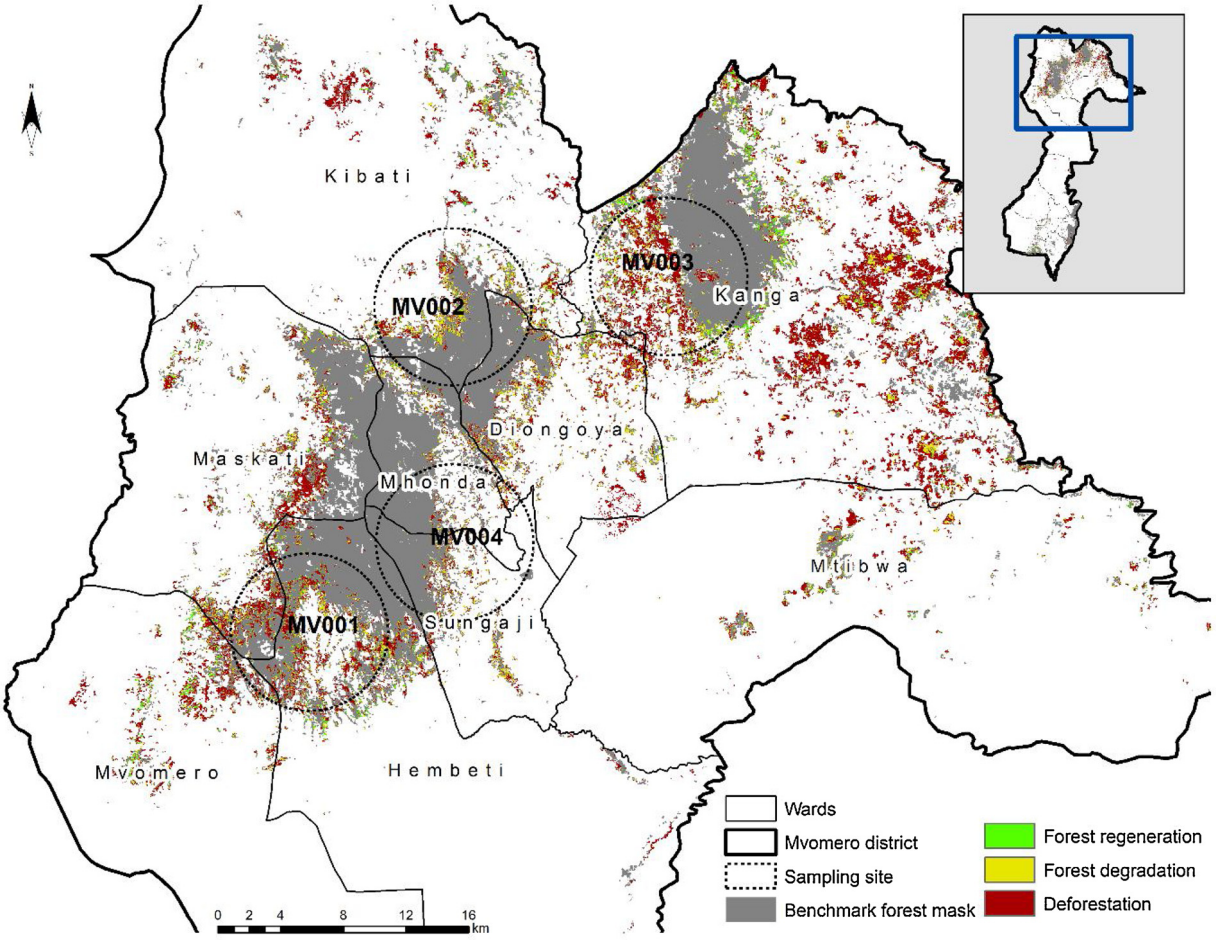

Fig. 8. Deforestation, forest degradation and regeneration in the Mvomero District, Tanzania as detected from Landsat time series (2001–2017) using STEF (Space-time Extremes and Features) algorithm (Hamunyela et al., 2017).

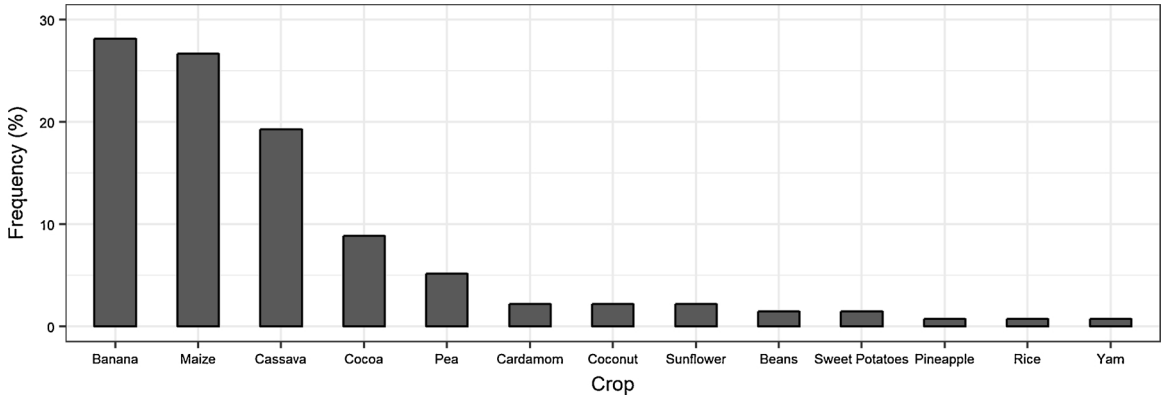

Fig. 9. Crops grown on deforested areas at the sampled locations in the Mvomero District, Tanzania, and their frequency of occurrence.

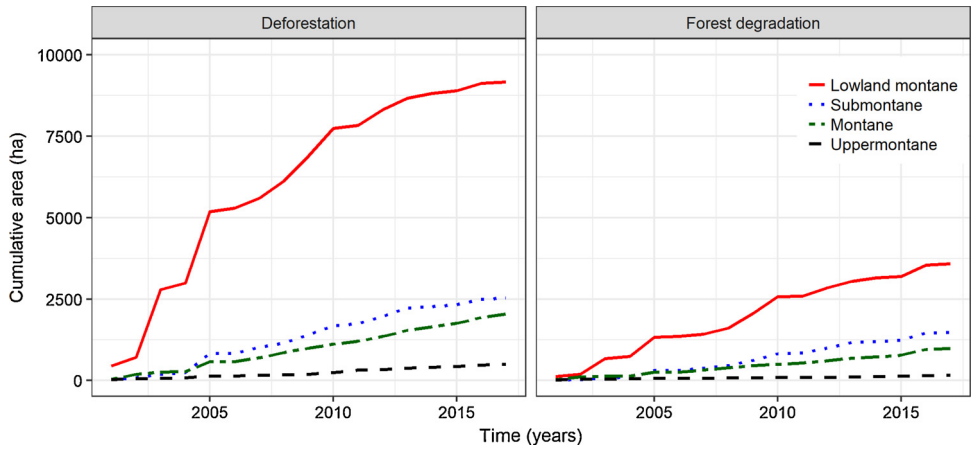

Fig. 10. Temporal cumulative area of deforestation and forest degradation by elevation zone in the Mvomero District, Tanzania, as detected from Landsat time series (2001–2017) using STEF (Space-time Extremes and Features) algorithm (Hamunyela et al., 2017).

forest cover to cultivate. Activities such as firewood extraction, charcoal production and timber harvesting might also have contributed to forest degradation. These activities are frequent drivers behind forest degradation in many African forest landscapes (Dresen et al., 2014; Pratihast et al., 2014), and known to be common in Mvomero District (Lyimo, 2014).

Only a small proportion (9 %) of disturbed forest in the Mvomero District between 2001 and 2017 was able to regenerate (Fig. 8). Several factors can explain the observed low regeneration rates. First, shifting cultivation practices, known to occur in this area (Mwampamba and Schwartz, 2011) have probably become rarer due to increased population. Therefore, deforested areas converted to cropland might have remained cropland permanently. Higher population means less land for everyone, therefore, no land available to put some of it into fallows. Second, we found evidence of grazing and browsing at some sample locations. Continuous grazing and browsing by livestock might also suppressed forest regeneration.

At least 12 % of all forest disturbances that occurred in Mvomero District between 2001 and 2017 happened within areas designated as forest reserves (1034 ha) and national park/nature reserve (1425 ha). Deforestation (70 %) dominated the disturbances that occurred within the forest reserves and national park/nature reserves. However, 76 % of disturbances in forest reserves and national park/nature reserves happened between 2001 and 2010, with the remaining 24 % occurring during 2011–2017 period. These results show that clearance and degradation of forest in Mvomero District within forest reserves and national park/ nature reserves is relatively limited, and has decreased sharply in recent years (2011–2017). This decline in forest disturbance within the forest reserves and national park/nature reserves could be a result of recent effort to eliminate farms encroaching into forest reserve. However, continued occurrence of forest disturbances, particularly deforestation within forest reserves highlights the presence of a loophole in the current mechanisms for protecting forests in this area. We found 9 % of regenerated forest in Mvomero District to have occurred within the forest reserves (83 ha) and national park/nature reserve (82 ha). We expected most forest regeneration to occur within forest reserves and national park/nature reserves because of the abandonment of farms that encroached into forest reserves. This limited regeneration within the forest reserves and national park/nature reserve may be due to the fact that most of the disturbed were cleared for cropland. Re-establishment of a forest on an abandoned cropland is likely to take a longer period.

4.2. Deforestation, forest degradation and regeneration along the elevational gradient

Most of the deforestation and forest degradation that occurred in Mvomero District between 2001 and 2017 were at lower elevation (lowland montane), with disturbance events decreasing as the elevation increases (Fig. 10). While the absolute value of disturbed area was lower at higher elevations, we observed an increasing trend in higher elevations in recent years (2011–2017). During the 2001–2010 period, more than 60 % of deforestation and forest degradation events occurred in lowland montane and less than 15 % of at high elevations (montane and uppermontane). In subsequent years (2011–2017), however, deforestation and forest degradation activities shifted to higher elevations (Fig. 11), declining sharply at low elevation. During this period, more than 50 % of deforestation and forest degradation activities were

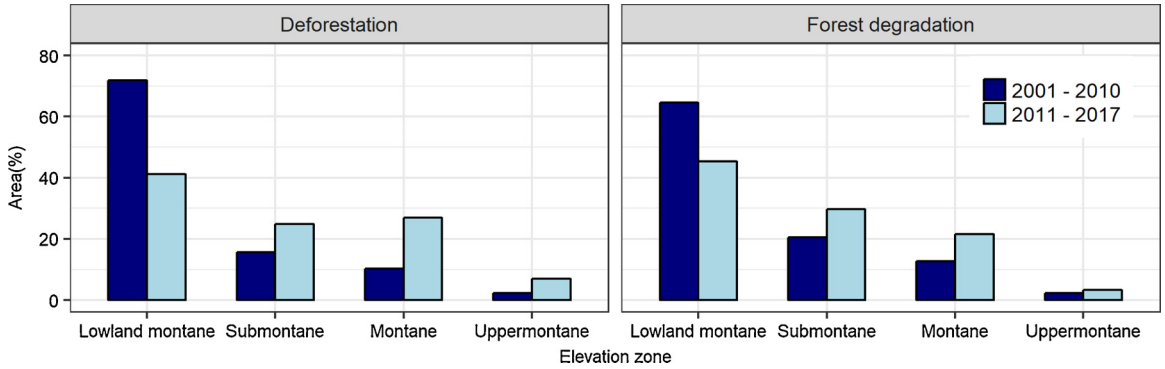

Fig. 11. Proportion of deforestation and forest degradation by elevation zone during the 2001–2010 and 2011–2017 in the Mvomero District, Tanzania.

occurring at elevations higher than > 800 m (submontane, montane and uppermontane). Note that the total deforested area is much greater than degraded forests, which explains the difference between values observed in Fig. 10 (raw area) and Fig. 11 (normalized by category). High elevation and existing forest conservation mechanisms (e.g. establishment of forest reserves) are not a strong barrier for forest disturbance in Mvomero District. Effective interventions are therefore needed to protect the key ecosystem services of these montane forests.

By area, most of the regeneration occurred at the lowland montane, but the highest regeneration success rate (11 %) was at submontane zone. Differences in regeneration between the elevation zones were nonetheless negligible (Fig. 12). Livestock grazing and browsing activities are likely to occur at low elevation because it might be less challenging for livestock to move around when compared to high elevations. Therefore, livestock grazing and browsing might have limited forest regeneration after disturbance at lower elevations. In addition, most forest degradation occurred at high elevations. Expectedly, degraded forest is likely to have higher regeneration than deforested areas.

4.3. The utility of global forest loss products for local forest assessment

Globally generated forest loss datasets (e.g. Hansen et al., 2013) are increasingly being used for local forest loss assessment as baseline forest change scenarios (Hojas-Gascon et al., 2015), but the utility of such products is often not assessed. Our map-to-map comparison approach show that the global forest loss dataset (Hansen et al., 2013) underestimated forest loss in Mvomero District with a large margin (Fig. 13). Forest loss estimates from the global dataset were two times lower than what was detected by our locally calibrated algorithm. Our algorithm detected over 10,000 ha of forest loss (13 % of the total forest cover in Mvomero District) more than the global dataset. This difference should however be interpreted with care because our validation for deforestation did not cover the entire study area. The only validation that covered the whole study area was for forest disturbance (without discriminating between deforestation and degradation). The global dataset nonetheless missed many obvious forest clearances, especially at high elevations. In our study area, forest disturbances occurred at small spatial scale. Therefore, the underestimation of forest loss by the global product is not surprising. However, the margin of underestimation is surprisingly high. We therefore do not recommend the use of global forest loss datasets for local forest loss assessment, including accounting of forest related GHG emissions in montane forest landscapes of Tanzania. To improve current global estimates of forest related GHG emissions, there is an urgent need to improve the detection of forest disturbances and regeneration in forested landscapes with strong seasonality and in areas dominated by small-scale disturbances. New generation of forest change detection algorithms (e.g. STEF), which consider both spatial and temporal context, offer opportunities to improve detection of forest disturbances and regeneration in such areas (Brandt et al., 2018). Applying these algorithms to freely available data from satellite sensors with improved spatial resolution (10 m) and high revisiting frequency such as the Sentinel-1 and 2 sensors could further enhance detection of forest disturbances in complex forest landscapes. However, computationally powerful platforms (e.g. Google Engine Engine) would be needed in order to apply these algorithms to large areas.

5. Conclusion

Montane forests in Mvomero District, Tanzania, underwent forest disturbances (20 487 ha) between 2001 and 2017. The disturbances are

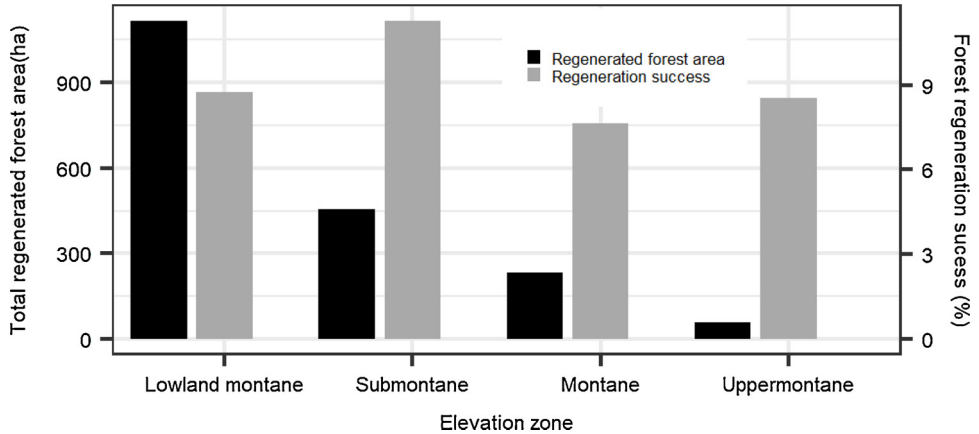

Fig. 12. Regenerated forest area and forest regeneration success after disturbance by elevation in the Mvomero District, Tanzania, during the 2001–2017 period. Forest regeneration was detected from Landsat time series (2001–2017) using STEF (Space-time Extremes and Features) algorithm (Hamunyela et al., 2017).

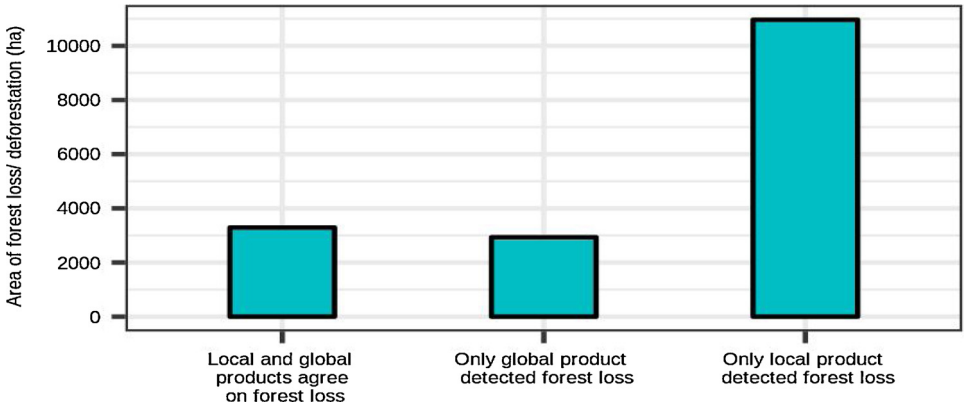

Fig. 13. Map-to-map agreement and disagreement between deforestation detected by STEF algorithm (Hamunyela et al., 2017) and global forest loss product (Hansen et al., 2013) in Mvomero District, Tanzania. Deforestation and global forest loss products were derived from Landsat time series (2001–2017).

dominated by deforestation. Forest disturbances have been occurring mainly at lowland montane between 2000 and 2010, but are increasingly shifting to higher elevations in recent years (2011–2017). Forest clearance to establish small-scale crop farming is driving forest disturbances in species-rich montane forest landscapes of Mvomero District in Tanzania. Given high dependence on agriculture in the Mvomero District, reducing forest disturbance would require integrated land use policies that take the livelihood of local communities around the montane forests and the benefits derived from forest conservation into consideration. Sustainable agricultural intensification could be one of the critical approaches to reduce forest clearance driven by cropland expansion. Without sustainable agricultural intensification to increase the yields of smallholder farming in order to meet the food demand of a growing population, the risk for montane forests to disappear through deforestation in near future might increase. Natural forest regeneration in these montane forests is marginal, and may not be relied upon to counteract the impact of forest disturbance. To prevent the unmitigated loss of montane forests in Mvomero District, efforts such as community-driven forest restoration should be considered.

Globally generated forest loss datasets grossly underestimate forest loss in these montane landscapes, and cannot be relied upon for regular assessment of forest changes in these areas. New generation of approaches for detecting changes in forest cover which combine spatial and temporal context in satellite data offer opportunity to improve forest monitoring in forest landscapes where hard-to-detect small-scale disturbances are common and can be used for regular assessment of forest changes. Improving the detection of small-scale forest disturbances will improve the global estimates of forest related GHG emissions, but greater improvement will be realised when forest regeneration is fully incorporated in forest change assessments.

Author statement

E. H., R. M. R-C, M. H and **P. B** conceived of the presented idea. E.H performed the computations and data analysis. **R. M. R-C, E. H** and **D. S** supported the field data collection, and **H.T.T.D** contributed to the literature review. All authors discussed the results and contributed to the final manuscript.

Declaration of Competing Interest

The authors declare that they have no known competing financial interests or personal relationships that could have appeared to influence the work reported in this paper.

Acknowledgements

This research was implemented thanks to the generous support from IFAD (International Funds for Agricultural Development) and CCAFs (CGIAR Program on Climate Change, Agriculture and Food Security). Our gratitude goes to IITA (International Institute of Tropical Agriculture) and Sokoine University of Agriculture in Morogoro for supporting the groundtruthing work of this research. We are thankful to the anonymous reviewers whose comments greatly improved this manuscript.

Appendix A. Supplementary data

Supplementary material related to this article can be found, in the online version, at doi:https://doi.org/10.1016/j.jag.2020.102063.

References

Achard, F., Beuchle, R., Mayaux, P., Stibig, H.-J., Bodart, C., Brink, A., et al., 2014. Determination of tropical deforestation rates and related carbon losses from 1990 to2010. Glob. Chang. Biol. 20, 2540–2554. https://doi.org/10.1111/gcb.12605.

Brandt, P., Hamunyela, E., Herold, M., de Bruin, S., Verbesselt, J., Rufino, M.C., 2018. Sustainable intensification of dairy production can reduce forest disturbance in Kenyan montane forests. Agric. Ecosyst. Environ. 265. https://doi.org/10.1016/j.agee.2018.06.011.

Breiman, L., 2001. Random forests. Mach. Learn. 45, 5–32. https://doi.org/10.1007/9781441993267_5.

Burgess, N.D., Butynski, T.M., Cordeiro, N.J., Doggart, N.H., Fjeldsa, J., Kilahama, F.B., et al., 2007. The biological importance of the Eastern Arc Mountains of Tanzania and Kenya. Biol. Conserv. 134, 209–231. https://doi.org/10.1016/j.biocon.2006.08.015.

Carter, S., Herold, M., Rufino, M.C., Neumann, K., Kooistra, L., Verchot, L., 2015. Mitigation of agricultural emissions in the tropics: comparing forest land-sparing options at the national level. Biogeosciences 12 (15), 4809–4825. https://doi.org/10.5194/bg-12-4809-2015.

Chaverri, G., Garin, I., Alberdi, A., Jimenez, L., Castillo-Salazar, C., Aihartza, J., 2016. Unveiling the hidden bat diversity of a neotropical montane forest. PLoS One 11 (10). https://doi.org/10.1371/journal.pone.0162712.

Cohen, W.B., Yang, Z., Kennedy, R., 2010. Detecting trends in forest disturbance and recovery using yearly Landsat time series: 2. TimeSync - Tools for calibration and validation. Remote Sens. Environ. 114 (12), 2911–2924. https://doi.org/10.1016/j.rse.2010.07.010.

Devries, B., Decuyper, M., Verbesselt, J., Zeileis, A., Herold, M., Joseph, S., 2015a. Tracking disturbance-regrowth dynamics in tropical forests using structural change detection and Landsat time series. Remote Sens. Environ. 169, 320–334. https://doi.org/10.1016/j.rse.2015.08.020.

DeVries, B., Verbesselt, J., Kooistra, L., Herold, M., 2015b. Robust monitoring of small-scale forest disturbances in a tropical montane forest using Landsat time series. Remote Sens. Environ. 161, 107–121. https://doi.org/10.1016/j.rse.2015.02.012.

Doggart, N., Loserian, D. (Eds.), 2007. South Nguru Mountains: A Description of the Biophysical Landscape. Tanzania Forest Conservation Group Technical Paper No11. Dar es Salaam, Tanzania.

Dresen, E., DeVries, B., Herold, M., Verchot, L., Müller, R., 2014. Fuelwood savings and carbon emission reductions by the use of improved cooking stoves in an Afro-montane Forest, Ethiopia. Land 3 (3), 1137–1157. https://doi.org/10.3390/land3031137.

Fisher, B., 2010. African exception to drivers of deforestation Misrepresentation of the IPCC CO 2 emission scenarios. Nature Publ. Group 3 (6), 375–376. https://doi.org/10.1038/ngeo873.

Gao, B., 1996. NDWI - A normalised difference water index for remote sensing of vegetation liquid water from space. Remote Sens. Environ. 58 (3), 257–266.

Gerland, P., Li, N., Gu, D., Spoorenberg, T., Alkema, L., Fosdick, B.K., et al., 2014. World

population stabilization unlikely this century. Science 346 (6206).
Hall, J., Burgess, N.D., Lovett, J., Mbilinyi, B., Gereau, R.E., 2009. Conservation implications of deforestation across an elevational gradient in the Eastern Arc Mountains, Tanzania. Biol. Conserv. 142 (11), 2510–2521. https://doi.org/10.1016/j.biocon.2009.05.028.
Hamunyela, E., Verbesselt, J., Bruin, S., Herold, M., 2016a. Monitoring deforestation at sub-annual scales as extreme events in landsat data cubes. Remote Sens. 8 (8). https://doi.org/10.3390/rs8080651.
Hamunyela, E., Verbesselt, J., Herold, M., 2016b. Using spatial context to improve early detection of deforestation from Landsat time series. Remote Sens. Environ. 172. https://doi.org/10.1016/j.rse.2015.11.006.
Hamunyela, E., Reiche, J., Verbesselt, J., Herold, M., 2017. Using space-time features to improve detection of forest disturbances from Landsat time series. Remote Sens. 9 (6). https://doi.org/10.3390/rs9060515.
Hansen, M.C., Potapov, P.V., Moore, R., Hancher, M., Turubanova, S.A., Tyukavina, A., et al., 2013. High-resolution global maps of 21st-century forest cover change. Science 342 (6160), 850–853. https://doi.org/10.1126/science.1244693.
Hartigan, J., 1975. Clustering Algorithms. A. Hartigan-Clustering Algorithms-John Wiley & Sons Retrieved from (1975).pdf. http://people.inf.elte.hu/fekete/algoritmusok_msc/klaszterezes/John.
Hojas-Gascon, L., Cerutti, P.O., Eva, H., Nasi, R., Martius, C., 2015. Monitoring Deforestation and Forest Degradation in the Context of REDD+: Lessons from Tanzania. https://doi.org/10.17528/cifor/005642.
Hosonuma, N., Herold, M., De Sy, V., De Fries, R.S., Brockhaus, M., Verchot, L., et al., 2012. An assessment of deforestation and forest degradation drivers in developing countries. Environ. Res. Lett. 7 (4). https://doi.org/10.1088/1748-9326/7/4/044009.
Jacobs, S.R., Breuer, L., Butterbach-Bahl, K., Pelster, D.E., Rufino, M.C., 2017. Land use affects total dissolved nitrogen and nitrate concentrations in tropical montane streams in Kenya. Sci. Total Environ. 603–604, 519–532. https://doi.org/10.1016/j.scitotenv.2017.06.100.
Liaw, A., Wiener, M., 2002. Classification and regression by randomForest. R News 2 (3) 18–12. Retrieved from. https://cran.r-project.org/doc/Rnews/.
Lovett, J.C., 1998. Continuous change in Tanzanian moist forest tree communities with elevation. J. Trop. Ecol. 14, 719–722.
Lovett, J.C., Moyer, D.C., 1992. A new nature reserve in the Eastern Arc mountains, Tanzania. Oryx 26, 115–118.
Lovett, J.C., Clarke, G.P., Moore, R., Morrey, G.H., 2001. Elevational distribution of restricted range forest tree taxa in eastern Tanzania. Biodivers. Conserv. 10 (4), 541–550. https://doi.org/10.1023/A:1016610526242.
Lyimo, E., 2014. An Analysis of the Stakeholders and Drivers of Deforestation and Forest Degradation in the South Nguru Landscape. TFCG Technical Paper 45. TFCG, DSM, TZ, pp. 1–59.
Masek, J.G., Vermote, E.F., Saleous, N.E., Wolfe, R., Hall, F.G., Huemmrich, K.F., et al., 2006. A landsat surface reflectance dataset for North America, 1990-2000. IEEE Geosci. Remote. Sens. Lett. 3 (1), 68–72.
Milodowski, D.T., TAMitchard, E., Williams, M., 2017. Forest loss maps from regional satellite monitoring systematically underestimate deforestation in two rapidly changing parts of the Amazon. Environ. Res. Lett. 12, 094003. https://doi.org/10.1088/1748-9326/aa7e1e.
Mwampamba, T.H., Schwartz, M.W., 2011. The effects of cultivation history on forest recovery in fallows in the Eastern Arc Mountain, Tanzania. For. Ecol. Manage. 261 (6), 1042–1052. https://doi.org/10.1016/j.foreco.2010.12.026.
Myers, N., Mittermeier, R.A., Mittermeier, C.G., da Fonseca, G.A.B., Kent, J., 2000. Biodiversity hotspots for conservation priorities. Nature 403, 853–858.
Newmark, W.D., 2002. Conserving Biodiversity in East African Forests: a Study of the Eastern Arc Mountains. Ecological Studies, vol. 155. Springer-Verlag, Berlin, Germany, pp. 197.
Olofsson, P., Foody, G.M., Herold, M., Stehman, S.V., Woodcock, C.E., Wulder, M.A., 2014. Good practices for estimating area and assessing accuracy of land change. Remote Sens. Environ. 148, 42–57. https://doi.org/10.1016/j.rse.2014.02.015.
Pócs, T., Temu, R.P.C., Minja, T.R.A., 1990. Survey of natural vegetation and flora of the NguruMountains. In: Hedberg, I., Perssson, E. (Eds.), Research for Conservation of Tanzanian Catchment Forests, Proceedings from a Workshop Held in Morogoro, Tanzania. Uppsala, Sweden, pp. 135–149 March 13–17, 1989.
Pratihast, A.K., DeVries, B., Avitabile, V., de Bruin, S., Kooistra, L., Tekle, M., Herold, M., 2014. Combining satellite data and community-based observations for forest monitoring. Forests 5 (10), 2464–2489. https://doi.org/10.3390/f5102464.
Raben, K., Nyingi, J., Loserian, D., Akello, Z., Kidoido, M., 2006. Identifying Local Stakeholders in Forest Landscapes: Understanding the Use of Ecological Goods Kasyoha - Kitomi Landscape, Uganda Nguru South Landscape. Tanzania. Tanzania Forest Conservation Group.
Redhead, J.F., 1981. The Mazumbai Forest: an island of lower montane rainforest in the West Usambaras. Afr. J. Ecol. 19, 195–199.
Roy, D.P., Kovalskyy, V., Zhang, H.K., Vermote, E.F., Yan, L., Kumar, S.S., Egorov, A., 2016. Characterization of Landsat-7 to Landsat-8 reflective wavelength and normalized difference vegetation index continuity. Remote Sens. Environ. 185, 57–70. https://doi.org/10.1016/j.rse.2015.12.024.
Särkinen, T., Pennington, R.T., Lavin, M., Simon, M.F., Hughes, C.E., 2012. Evolutionary islands in the Andes: persistence and isolation explain high endemism in Andean dry tropical forests. J. Biogeogr. 39 (5), 884–900. https://doi.org/10.1111/j.1365-2699.2011.02644.x.
Schmidt, G., Jenkerson, C., Masek, J., Vermote, E., Gao, F., 2013. Landsat Ecosystem Disturbance Adaptive Processing System (LEDAPS) Algorithm Description.
Schmitt, C.B., Denich, M., Demissew, S., Friis, I., Boehmer, H.J., 2010. Floristic Diversity in Fragmented Afro-montane Rainforests: Altitudinal Variation and Conservation Importance. pp. 291–304. https://doi.org/10.1111/j.1654-109X.2009.01067.x.
Stehman, S.V., 2009. Sampling designs for accuracy assessment of land cover. Int. J. Remote Sens. 30 (20), 5243–5272. https://doi.org/10.1080/01431160903131000.
Stehman, S.V., Olofsson, P., Woodcock, C.E., Herold, M., Friedl, M.A., 2012. A global land-cover validation data set, II: augmenting a stratified sampling design to estimate accuracy by region and land-cover class. Int. J. Remote Sens. 33 (22), 6975–6993. https://doi.org/10.1080/01431161.2012.695092.
Tobey, J., 2008. A Profile of the Wami River Sub-Basin. A Report Prepared for the Tanzania Coastal Management Partnership for Sustainable Coastal Communities and Ecosystems in Tanzania.
Tropek, R., Sedláček, O., Beck, J., Keil, P., Musilová, Z., Šímová, I., Storch, D., 2014. Comment on 'high-resolution global maps of 21st-century forest cover change'. Science 344–981.
Tyukavina, A., Hansen, M.C., Potapov, P., Parker, D., Okpa, C., Stehman, S.V., et al., 2018. Congo Basin forest loss dominated by increasing smallholder clearing. Sci. Adv. 4 (11). https://doi.org/10.1126/sciadv.aat2993. eaat2993.
UNEP-WCMC, 2019. Protected Area Profile for United Republic of Tanzania from the World Database of Protected Areas, November 2019. Available at:. www.protectedplanet.net.
United Nations, 2017. World Population Prospects: The 2017 Revision. Retrieved from. https://population.un.org/wpp.
United Republic of Tanzania, 2011. Southern agricultural growth investment blueprint. Southern Agricultural Growth Corridor of Tanzania - Investment Blueprint. Retrieved from. http://www.sagcot.com/who-we-are/what-is-sagcot/.
United Republic of Tanzania, 2018. Tanzania Forest Reference Emission Level Submission to the UNFCCC.h. Retrieved from. ttps://redd.unfccc.int/files/frel_for_tanzania_december2016_27122016.pdf.
Verbesselt, J., Zeileis, A., Herold, M., 2012. Near real-time disturbance detection using satellite image time series. Remote Sens. Environ. 123, 98–108. https://doi.org/10.1016/j.rse.2012.02.022.
Vermote, E., Justice, C., Claverie, M., Franch, B., 2016. Preliminary analysis of the performance of the Landsat 8/OLI land surface reflectance product. Remote Sens. Environ. 185, 46–56. https://doi.org/10.1016/j.rse.2016.04.008.
Zhu, Z., 2017. Change detection using landsat time series: a review of frequencies, preprocessing, algorithms, and applications. ISPRS J. Photogramm. Remote. Sens. 130, 370–384.
Zhu, Z., Woodcock, C.E., 2012. Object-based cloud and cloud shadow detection in Landsat imagery. Remote Sens. Environ. 118, 83–94. https://doi.org/10.1016/j.rse.2011.10.028.
Zhu, Z., Woodcock, C.E., 2014a. Automated cloud, cloud shadow, and snow detection in multitemporal Landsat data: an algorithm designed specifically for monitoring land cover change. Remote Sens. Environ. 152, 217–234. https://doi.org/10.1016/j.rse.2014.06.012.
Zhu, Z., Woodcock, C.E., 2014b. Continuous change detection and classification of land cover using all available Landsat data. Remote Sens. Environ. 144, 152–171. https://doi.org/10.1016/j.rse.2014.01.011.
Zhu, Z., Wang, S., Woodcock, C.E., 2015. Improvement and expansion of the Fmask algorithm: Cloud, cloud shadow, and snow detection for Landsats 4-7, 8, and Sentinel 2 images. Remote Sens. Environ. 159, 269–277. https://doi.org/10.1016/j.rse.2014.12.014.